A Stochastic Planning Framework for Africa-Europe VSC-HVDC Renewable Electricity Trade: Security and Market Screening of an ELMED-Type Case

Adebayo V. Adeyinka[1], Samuel Oladeji[2]

[1]Dept. of Elect. Engineering, University of Cape Town, Cape Town, South Africa

[2]Dept. of Elect. Engineering, University of Strathclyde, UK

ABSTRACT

Africa-Europe high-voltage direct-current (HVDC) interconnectors are increasingly considered enabling infrastructure for renewable electricity export, regional adequacy support, and cross-border electricity market integration. This paper develops a two-stage stochastic planning framework for Africa-Europe renewable electricity trade in which corridor, converter, storage, and reinforcement decisions are separated from scenario-dependent dispatch. The framework combines AC/DC power-flow representation, VSC-HVDC converter limits, HVDC loss modelling, domestic adequacy protection, frequency-security screening, voltage and short-circuit-ratio screening, and loss-adjusted market-value calculations. A stylised ELMED-type Tunisia-Italy VSC-HVDC case is used only as a numerical screening benchmark; it is not presented as an official project model or a utility-grade simulation. The screening results indicate that a 600 MW VSC-HVDC corridor can reduce renewable curtailment, improve export utilisation, and create congestion-rent value when supported by storage and adequate converter control. They also show that transfer capacity alone is an inadequate planning criterion: grid strength, converter current limits, frequency-response capability, local adequacy requirements, cable availability, carbon value, and market-price spreads materially affect the technical and economic value of the corridor. The paper, therefore, positions the proposed model as an auditable planning-and-screening framework and identifies the additional data and RMS/EMT validation required for a final utility-grade submission.

Index Terms: AC/DC optimal power flow, Africa-Europe interconnection, congestion rent, frequency security, HVDC, market coupling, renewable export, stochastic planning framework, VSC-HVDC, voltage stability, weak-grid screening.

Nomenclature

Symbol	Meaning	Unit
Omega, omega	Scenario set and individual scenario for renewable output, demand, market price, and cable availability.	-
pi_omega	Probability of scenario omega.	-
T, N, L, G, K, C	Sets of time periods, AC buses, AC branches, generators, candidate HVDC corridors, and contingencies.	-
x_k, S_k	Corridor-build binary variable and installed converter apparent-power rating for corridor k.	-, MVA
E_B, P_B	Installed BESS energy and power ratings.	MWh, MW
P_s,k^send, P_s,k^rec	Scenario-dependent sending-end and receiving-end HVDC active powers.	MW
Q_s,k^conv, V_s,n, theta_s,n	Convert reactive power, AC voltage magnitude, and voltage angle.	MVAr, p.u., rad
SOC_s,t	Battery state of charge in scenario s and time t.	MWh
ENS_s,t	Energy not served; penalised to protect domestic adequacy.	MWh
SCR, ESCR	Short-circuit ratio and effective short-circuit ratio at the converter terminal.	-

INTRODUCTION

The decarbonisation of European electricity systems and the high solar and wind resource potential of North Africa create a credible engineering opportunity for renewable electricity exchange across the Mediterranean. The relevant planning problem, however, is not merely a matter of geographical routing. A secure and bankable Africa-Europe interconnector must be planned as an integrated AC/DC power system in which technical, economic, regulatory, and stability constraints are treated simultaneously.

HVDC transmission is attractive for long-distance submarine corridors because it avoids the charging-current limitations of long HVAC cables and provides controllable active-power exchange between weakly coupled or asynchronous AC systems. Voltage-source-converter HVDC (VSC-HVDC) is particularly relevant for renewable export corridors because the converter can provide active-power control, reactive-power control, voltage support, and selected grid-support functions at the terminal buses. Nevertheless, a VSC-HVDC corridor may also aggravate weak-grid interaction if converter controls, current limitation, phase-locked-loop dynamics, fault-ride-through logic, DC protection, and local AC reinforcements are not properly designed.

Representative Africa-Europe corridors define the practical envelope of the problem. The existing Spain-Morocco AC interconnection demonstrates cross-continental power exchange across the Strait of Gibraltar. The Tunisia-Italy ELMED project provides a near-term 600 MW VSC-HVDC benchmark. The Egypt-Greece GREGY project illustrates a larger Eastern Mediterranean corridor of approximately 3 GW. The Morocco-UK Xlinks concept represents an ultra-long renewable export corridor and therefore exposes the commercial and operational difficulty of large-scale renewable electricity trade.

Research Gap

The literature may be organised into five relevant streams: AC/DC expansion planning, stochastic transmission-expansion planning, VSC-HVDC weak-grid stability, HVDC-supported frequency response, and market coupling. AC/DC power-flow and converter models provide the electrical representation of VSC-HVDC links. Still, they often do not embed investment uncertainty, domestic adequacy floors, and market-value allocation in the same optimisation layer [17]-[19]. Stochastic planning studies address uncertainty in investment decisions, but many do not explicitly represent converter current limits, weak-grid screening, and HVDC pole-outage frequency constraints [12], [13], [21]-[23]. Converter-stability and weak-grid studies provide the control-level requirements, but they are usually not linked to long-term renewable-export economics [25], [27]. Frequency-support studies clarify inertia and fast-response requirements, yet they do not by themselves determine which corridor, converter rating, and storage portfolio should be built [20], [28], [29]. Market-coupling discussions quantify value but rarely enforce the full technical feasibility of the export-side system. The gap addressed here is therefore not the existence of HVDC planning or converter-stability models in isolation; it is the absence of a transparent modelling sequence that jointly screens investment, AC/DC operation, local adequacy, frequency security, weak-grid limits, and market value for Africa-Europe renewable electricity trade.

Contributions

The paper makes the following contributions:

1. It formulates a two-stage stochastic AC/DC expansion-planning framework for Africa-Europe renewable export corridors, explicitly distinguishing non-anticipative first-stage investment decisions from scenario-dependent second-stage dispatch decisions.

2. It embeds domestic adequacy protection in the export-side African system so that renewable export is not scheduled at the expense of local reliability.

3. It introduces frequency-security constraints for HVDC pole outage, renewable uncertainty, and BESS/HVDC-supported fast frequency response.

4. It provides voltage-security and weak-grid screening using converter P-Q capability, converter-current limits, and short-circuit-ratio assessment.

5. It links physical dispatch to market value using loss-adjusted congestion rent, price-spread sensitivity, carbon value, and investment-recovery indicators.

6. It uses a stylised ELMED-type numerical screening case to demonstrate the planning, voltage-security, frequency-security, and market-value indicators, while explicitly identifying the additional data and validation required for a reproducible utility-grade study.

Organisation

Section II summarises representative corridors and technology choices. Section III discusses HVDC technology selection and system architecture. Section IV formulates the stochastic AC/DC planning framework. Section V presents the frequency- and voltage-security screening models. Section VI gives the market-coupling and investment-recovery formulation. Section VII reports the stylised ELMED-type screening case. Section VIII discusses engineering implications. Section IX states the limitations and IEEE-style submission requirements. Section X concludes the paper.

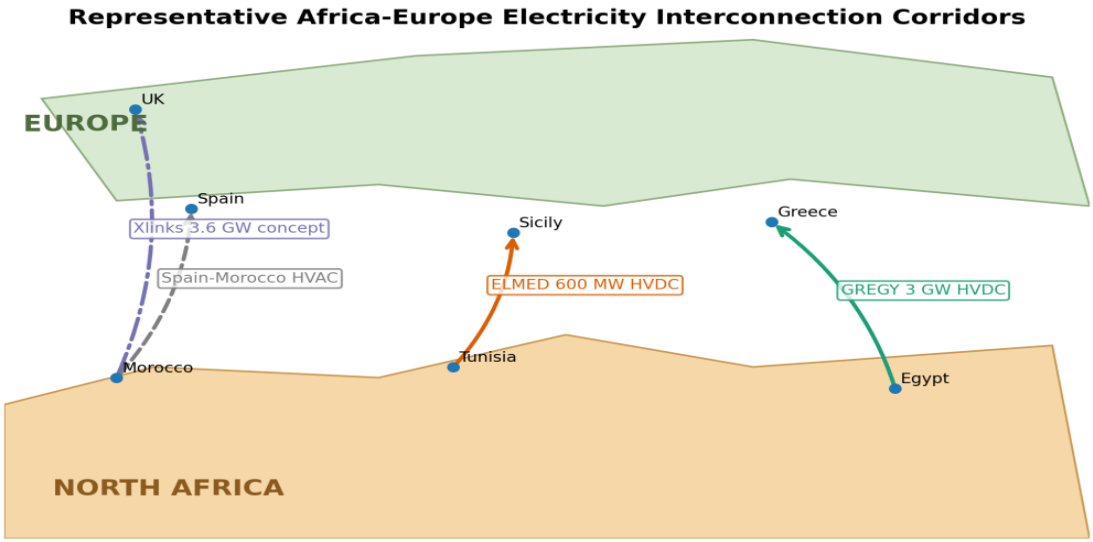


Fig. 1. *Representative Africa-Europe electricity interconnection corridors considered in planning studies.*

AFRICA-EUROPE HVDC CORRIDOR BACKGROUND

Table I summarises representative corridors used to motivate the planning model. The project webpages and press releases cited in this table are used only to identify public corridor facts such as indicative capacity, geography, and development status. They are not used as the technical basis of the proposed AC/DC optimisation or stability model. The technical foundation of the manuscript is instead drawn from peer-reviewed HVDC, AC/DC power-flow, stochastic planning, converter stability, and frequency control literature.

TABLE I. Representative Africa-Europe electricity interconnection corridors

Corridor/project	Technology	Indicative capacity	Indicative length	Engineering significance	Source
Spain-Morocco existing link	400 kV HVAC submarine AC interconnection	2 x 700 MW technical capacity	About 60 km across the Strait of Gibraltar	Existing Africa-Europe electricity exchange route; useful benchmark for interconnection operation.	[4], [5]

Tunisia-Italy ELMED	VSC-HVDC submarine interconnection	600 MW	About 200–224 km	Near-term Africa-Europe DC bridge and natural benchmark for renewable export and stability studies.	[1], [6]
Egypt-Greece GREGY	HVDC submarine interconnection	Up to 3000 MW	About 950–954 km	Large Eastern Mediterranean green-energy corridor with bidirectional capability.	[2], [3]
Morocco-UK Xlinks concept	Long-distance HVDC subsea export corridor	3.6 GW target	About 3800–4000 km	Stress test for ultra-long renewable export, firming, cable availability, and off take-bankability assumptions.	[7], [8]

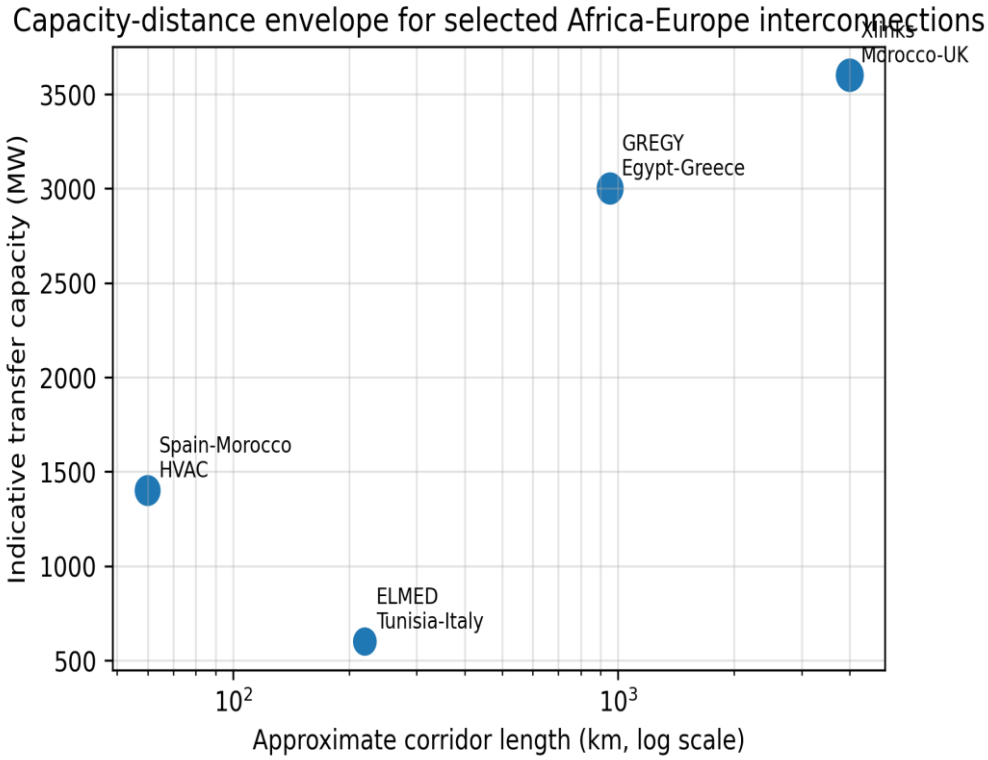


Fig. 2. *Indicative capacity-distance envelope of selected Africa-Europe interconnection examples.*

HVDC TECHNOLOGY SELECTION AND SYSTEM ARCHITECTURE

For submarine corridors of several hundred kilometres, HVDC is normally preferred to HVAC because cable charging current and reactive compensation become restrictive for AC operation. The choice between line-commutated-converter HVDC (LCC-HVDC) and VSC-HVDC should not be made on cost alone. The appropriate converter technology depends on AC-grid strength, fault level, harmonic performance, black-start requirements, reactive-power support, protection philosophy, and future multi-terminal expansion needs.

For renewable export corridors connected to relatively weak African collector grids, VSC-HVDC is a defensible baseline technology because it can independently control active and reactive power within converter current limits. This is not a claim of universal superiority over LCC-HVDC. The final technology choice depends on short-circuit strength, converter-control mode, current limitation, DC protection, harmonic filtering, losses, restoration requirements, multi-terminal expansion needs, and the strength of both terminal AC systems. If very high bulk transfer is required between two strong AC systems, LCC-HVDC may remain cost-competitive; for weak-grid renewable export and modular Mediterranean expansion, VSC-HVDC is

usually the more flexible screening assumption.

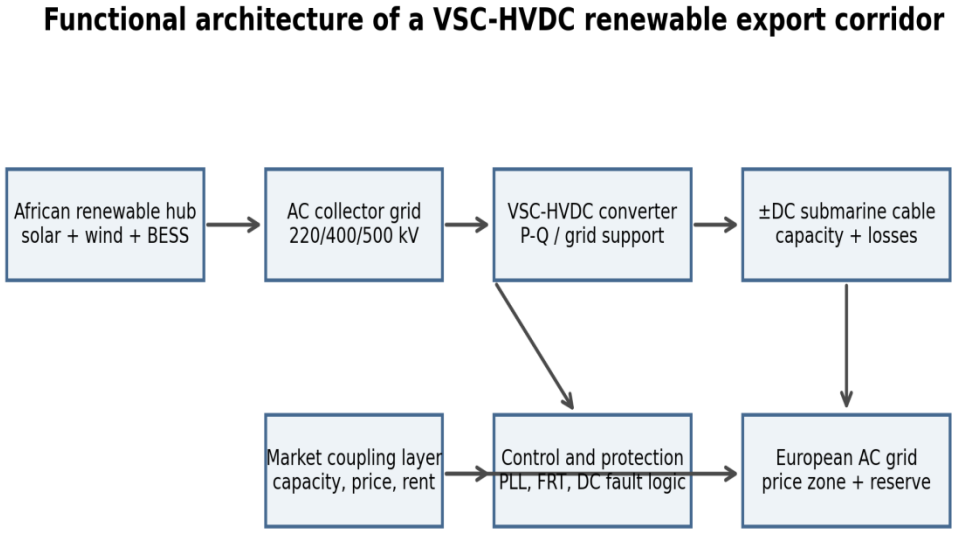


Fig. 3. *Functional architecture of a VSC-HVDC renewable export corridor with planning, control, and market layers.*

TABLE II. Technology comparison for submarine Africa-Europe interconnections

Criterion	HVAC submarine	LCC-HVDC	VSC-HVDC
Long-distance submarine suitability	Poor to moderate at short distances due to cable charging current.	Very good for high-power point-to-point bulk transfer.	Very good, especially for renewable export and future multi-terminal expansion.
Reactive power and voltage support	Requires compensation; reactive burden rises with length.	Consumes reactive power and requires filters/compensation.	Can provide dynamic reactive power and voltage support within converter limits.
Weak-grid compatibility	Limited by synchronism and voltage stability.	Poor unless short-circuit strength is high.	Good subject to PLL tuning, current limitation, and grid-forming/grid-following control choice.
Restoration and black-start support	Not inherent.	Limited.	Possible in selected grid-forming VSC configurations.
Best Africa-Europe application	Existing Strait of Gibraltar-type links.	Very large bulk transfer between strong grids.	Renewable export corridors require weak-grid support, modular expansion, and converter-based ancillary services.

PROPOSED STOCHASTIC AC/DC PLANNING MODEL

The planning model is formulated as the deterministic equivalent of a two-stage stochastic expansion-planning problem. First-stage decisions are made before the realisation of uncertainty in renewable generation, demand, market prices, and cable availability. Second-stage dispatch decisions are scenario-dependent. The first-stage variables are non-anticipative, i.e., the same investment decision is used across all scenarios. In a reproducible implementation, the scenario set must be generated from documented historical data or probability models, reduced using a stated scenario-reduction algorithm, assigned explicit probabilities, and published with the

optimisation input data. Without this information, the word stochastic would be merely decorative rather than auditable.

Scenario construction should preserve the correlation among renewable production, domestic demand, European and African market prices, and cable availability. A defensible implementation may use historical weather-demand-price traces, synthetic copula-based sampling, or clustered representative days. The reduced set Omega must include the probability pi_omega of each retained scenario and should be tested for sensitivity to the number of scenarios. First-stage corridor, converter, storage, and reinforcement decisions are common to all scenarios; generator dispatch, curtailment, BESS operation, ENS, market schedules, and corrective actions are scenario dependent.

Sets, Parameters, and Decision Variables

Let Ω denote the set of scenarios, with probability π_ω for each $\omega \in \Omega$, and let $\mathcal{T}$, $\mathcal{N}$, $\mathcal{L}$, $\mathcal{G}$, $\mathcal{K}$, and $\mathcal{C}$ denote the sets of time periods, AC buses, AC lines, generators, candidate HVDC corridors, and contingencies, respectively. The African export-side buses are collected in $\mathcal{N}^A$, while the European import-side buses are collected in $\mathcal{N}^E$.

First-stage investment variables are $x_k \in \{0,1\}$, S_k^{conv}, E^{BESS}, $P^{\text{BESS,max}}$, and r_n, denoting the build decision for candidate corridor k, converter MVA rating, storage energy rating, storage power rating, and AC reinforcement at bus or corridor n, respectively. Scenario-dependent operational variables include generator output $P_{gt\omega}$, bus voltage $V_{nt\omega}$, voltage angle $\theta_{nt\omega}$, AC branch flow $S_{\ell t\omega}$, HVDC sending and receiving powers $P_{kt\omega}^{\text{send}}$ and $P_{kt\omega}^{\text{rec}}$, converter reactive power $Q_{kt\omega}^{\text{conv}}$, renewable curtailment $P_{nt\omega}^{\text{curt}}$, battery charge and discharge $P_{t\omega}^{\text{ch}}$ and $P_{t\omega}^{\text{dis}}$, state of charge $E_{t\omega}^{\text{BESS}}$, and energy-not-served $ENS_{t\omega}$.

Objective Function

The two-stage stochastic planning objective minimises annualised investment cost plus expected operating cost and security penalties:

$$\min_{x,r,S^{\text{conv}},E^{\text{BESS}},P^{\text{BESS,max}},y_\omega} Z = \sum_{k\in\mathcal{K}} C_k^{\text{inv}}\, x_k + \sum_{n\in\mathcal{N}} C_n^{\text{rein}}\, r_n + C_E^{\text{BESS}} E^{\text{BESS}} + C_P^{\text{BESS}} P^{\text{BESS,max}} + \sum_{\omega\in\Omega} \pi_\omega\, Q(x,\omega) \tag{1}$$

where the second-stage cost is

$$Q(x,\omega) = \sum_{t\in\mathcal{T}} \Delta t \Big[\sum_{g\in\mathcal{G}} C_g\left(P_{gt\omega}\right) + C^{\text{curt}} \sum_{n\in\mathcal{N}} P_{nt\omega}^{\text{curt}} + VOLL\, ENS_{t\omega} + C^{\text{loss}} \sum_{k\in\mathcal{K}} P_{kt\omega}^{\text{loss}}\Big]. \tag{2}$$

The first-stage term includes annualised costs of corridor construction, converter MVA rating, BESS energy and power rating, and AC reinforcement. The second-stage term includes fuel or production costs, renewable curtailment penalty, energy not served penalty, BESS cycling or degradation costs where relevant, and the operating value or penalty associated with carbon and market schedules. Annualisation should state the discount rate, asset lifetime, and fixed operation and maintenance assumptions. ENS must be penalised by a value of lost load large enough to prevent artificial export at the expense of domestic reliability.

If a quadratic production-cost curve represents generation cost, then

$$C_g\left(P_{gt\omega}\right) = a_g u_{gt\omega} + b_g P_{gt\omega} + c_g P_{gt\omega}^2, \qquad g \in \mathcal{G},\ t \in \mathcal{T},\ \omega \in \Omega. \tag{3}$$

AC Network Constraints

For a full AC representation, active and reactive nodal balances are imposed at each bus. Let G_{nm} and B_{nm} be the real and imaginary parts of the AC admittance matrix, and $\theta_{nm,t\omega} = \theta_{nt\omega} - \theta_{mt\omega}$. The active and reactive power injected from bus n into the AC network are

$$P_{nt\omega}^{\text{net}} = V_{nt\omega} \sum_{m\in\mathcal{N}} V_{mt\omega} \left(G_{nm}\cos\theta_{nm,t\omega} + B_{nm}\sin\theta_{nm,t\omega}\right), \quad (4)$$

$$Q_{nt\omega}^{\text{net}} = V_{nt\omega} \sum_{m\in\mathcal{N}} V_{mt\omega} \left(G_{nm}\sin\theta_{nm,t\omega} - B_{nm}\cos\theta_{nm,t\omega}\right). \quad (5)$$

The corresponding nodal active-power balance is

$$\sum_{g\in\mathcal{G}_n} P_{gt\omega} + P_{nt\omega}^{\text{RES,av}} - P_{nt\omega}^{\text{curt}} + P_{nt\omega}^{\text{dis}} - P_{nt\omega}^{\text{ch}} - P_{nt\omega}^{D} - P_{nt\omega}^{\text{HVDC}} - P_{nt\omega}^{\text{net}} + ENS_{nt\omega} = 0. \quad (6)$$

The reactive-power balance is

$$\sum_{g\in\mathcal{G}_n} Q_{gt\omega} + Q_{nt\omega}^{\text{conv}} + Q_{nt\omega}^{\text{sh}} - Q_{nt\omega}^{D} - Q_{nt\omega}^{\text{net}} = 0. \quad (7)$$

Voltage and line-flow constraints are

$$\underline{V}_n \le V_{nt\omega} \le \overline{V}_n, \qquad n \in \mathcal{N},\ t \in \mathcal{T},\ \omega \in \Omega, \quad (8)$$

$$|S_{\ell t\omega}| \le \overline{S}_\ell + r_\ell, \qquad \ell \in \mathcal{L},\ t \in \mathcal{T},\ \omega \in \Omega. \quad (9)$$

For large-scale planning studies, these nonlinear AC constraints may be replaced by a validated linearised AC/DC approximation. The approximation must be stated explicitly, for example, DC active-power flow with voltage/reactive-power screening, linearised AC power flow, or sequential AC/DC power flow. Any candidate corridor selected by the optimisation must then be checked using full AC power-flow analysis, converter-loading verification, N-1 post-contingency analysis, and dynamic simulation. The solver, version, hardware, optimality gap, and computation time should be reported with the numerical results.

VSC-HVDC Converter and DC-Cable Constraints

HVDC transfer is bounded by investment and converter rating:

The build-capacity logic must prevent dispatch through an unbuilt corridor. Therefore, the active-power transfer bounds, converter MVA limit, reactive-power capability, current limit, and loss model should all be multiplied or otherwise activated by the binary build variable x_k. If a continuous rating S_k is optimised, it must satisfy 0 <= S_k <= S_k^max x_k, so that both the investment and dispatch layers remain physically consistent.

$$-\overline{P}_k^{\text{HVDC}} x_k \le P_{kt\omega}^{\text{send}} \le \overline{P}_k^{\text{HVDC}} x_k, \qquad k \in \mathcal{K},\ t \in \mathcal{T},\ \omega \in \Omega. \quad (10)$$

Loss-adjusted receiving power is represented by

$$P_{kt\omega}^{\text{rec}} = P_{kt\omega}^{\text{send}} - P_{kt\omega}^{\text{loss}}, \quad (11)$$

$$P_{kt\omega}^{\text{loss}} = a_k x_k + b_k \left|P_{kt\omega}^{\text{send}}\right| + c_k \left(P_{kt\omega}^{\text{send}}\right)^2. \quad (12)$$

The converter P-Q capability is

$$(P_{kt\omega}^{\text{conv}})^2 + (Q_{kt\omega}^{\text{conv}})^2 \le (S_k^{\text{conv}})^2. \quad (13)$$

The current limit is imposed as

$$\sqrt{(P_{kt\omega}^{\text{conv}})^2 + (Q_{kt\omega}^{\text{conv}})^2} \le \sqrt{3}\, V_{kt\omega}^{\text{ac}} I_k^{\max}. \quad (14)$$

DC-side voltage and current limits are

$$\underline{V}_k^{\text{dc}} x_k \le V_{kt\omega}^{\text{dc}} \le \overline{V}_k^{\text{dc}} x_k, \qquad \left|I_{kt\omega}^{\text{dc}}\right| \le \overline{I}_k^{\text{dc}} x_k. \quad (15)$$

Renewable and BESS Constraints

Renewable utilisation and curtailment satisfy

$$0 \le P_{nt\omega}^{\mathrm{RES,av}} - P_{nt\omega}^{\mathrm{curt}} \le P_{nt\omega}^{\mathrm{RES,av}}, \qquad 0 \le P_{nt\omega}^{\mathrm{curt}} \le P_{nt\omega}^{\mathrm{RES,av}}. \tag{16}$$

The BESS state-of-charge dynamics are

$$E_{t\omega}^{\mathrm{BESS}} = E_{t-1,\omega}^{\mathrm{BESS}} + \eta^{\mathrm{ch}} P_{t\omega}^{\mathrm{ch}} \Delta t - \frac{P_{t\omega}^{\mathrm{dis}} \Delta t}{\eta^{\mathrm{dis}}}. \tag{17}$$

Storage energy and power bounds are

The BESS model should include charging and discharging efficiencies, initial and terminal SOC conditions, SOC limits, and links between dispatch variables and installed power and energy ratings. Simultaneous charging and discharging should be prevented by a binary operating-mode variable or justified through a convex relaxation when round-trip efficiency is below unity, and prices/penalties make simultaneous operation suboptimal.

$$\underline{E}^{\mathrm{BESS}} \le E_{t\omega}^{\mathrm{BESS}} \le E^{\mathrm{BESS}}, \tag{18}$$

$$0 \le P_{t\omega}^{\mathrm{ch}} \le P^{\mathrm{BESS,max}}, \qquad 0 \le P_{t\omega}^{\mathrm{dis}} \le P^{\mathrm{BESS,max}}. \tag{19}$$

Domestic Adequacy and Export-Protection Constraint

A renewable export corridor must not reduce the reliability of the exporting African system. The export schedule is therefore constrained by a domestic adequacy floor that can be represented as a minimum local supply margin, a minimum reserve requirement, an expected energy not served limit, or a policy-imposed export cap. In the stylised case, the adequacy floor is interpreted as a minimum domestic reserve margin that must remain available before export is scheduled:

$$\sum_{n \in \mathcal{N}^A} \left[\sum_{g \in \mathcal{G}_n} P_{gt\omega} + P_{nt\omega}^{\mathrm{RES,av}} - P_{nt\omega}^{\mathrm{curt}} + P_{nt\omega}^{\mathrm{dis}} - P_{nt\omega}^{\mathrm{ch}} - P_{nt\omega}^{D} \right] - P_{t\omega}^{\mathrm{export}} + P_{t\omega}^{\mathrm{import}} + ENS_{t\omega} \ge R_{t\omega}^{\mathrm{req}}. \tag{20}$$

This constraint prevents the export corridor from absorbing the local adequacy margin. Its data source, units, time resolution, and relationship to domestic load growth must be stated. The constraint is not merely political language; it is a power-system security condition that prevents a renewable-export project from degrading local reliability.

N-1 Security Constraints

For each credible contingency c in the contingency set C, branch and converter limits are enforced as

$$\left| S_{\ell t\omega}^{(c)} \right| \le \overline{S}_{\ell} + r_{\ell}, \qquad \ell \in \mathscr{L},\ c \in \mathcal{C}, \tag{21}$$

$$\left| P_{kt\omega}^{\mathrm{send,(c)}} \right| \le \overline{P}_{k}^{\mathrm{HVDC}} x_k, \qquad k \in \mathcal{K},\ c \in \mathcal{C}. \tag{22}$$

HVDC-pole outage is included as a high-impact contingency. Candidate corridors that pass only base-case power flow but fail N-1 transfer, voltage, or frequency requirements are rejected.

The contingency set should include the loss of one HVDC pole, the outage of critical AC export corridors, a converter transformer outage, a large renewable forecast error, BESS unavailability, and selected weak-grid disturbances. The paper must state whether post-contingency security is represented by full corrective redispatch, PTDF/LODF screening, sequential AC contingency analysis, or RMS dynamic simulation. N-1 security should not be claimed from unspecified constraints.

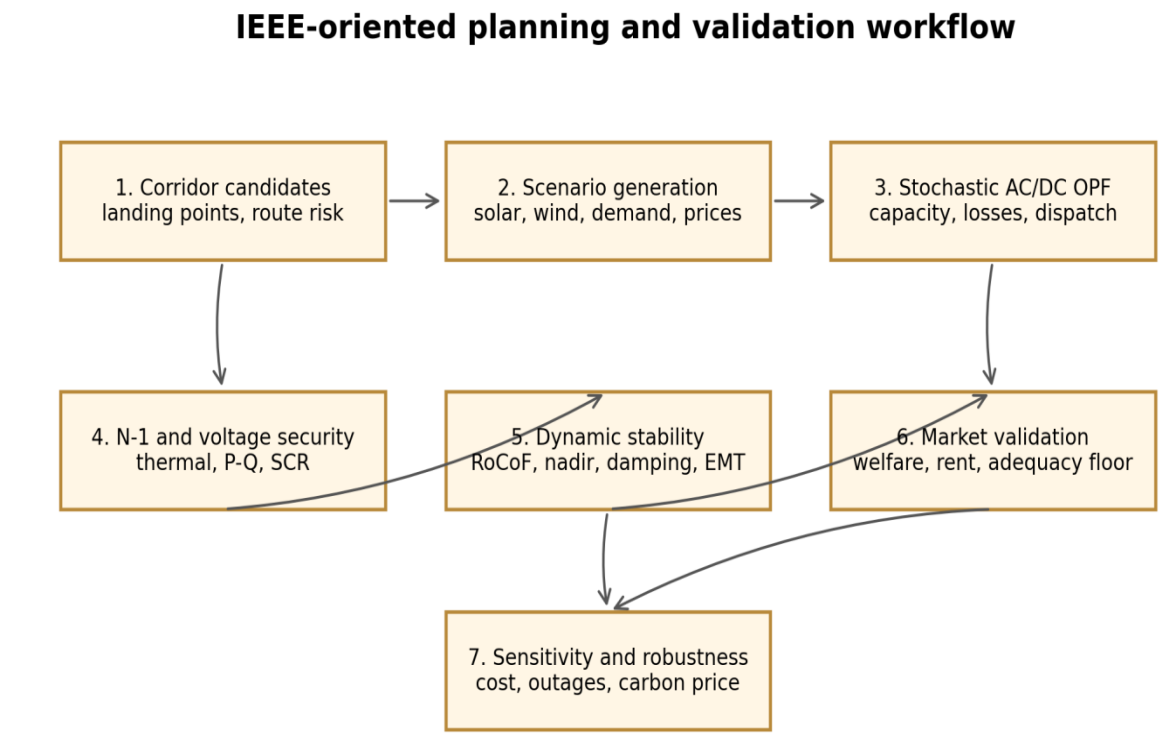


Fig. 4. *IEEE-oriented planning, power-flow, stability, and market-validation workflow.*

STABILITY ASSESSMENT MODEL

The planning solution is screened against stability requirements. In the present paper, this section is deliberately framed as a stability-screening model rather than a complete dynamic validation. It covers frequency response, voltage security margin, weak-grid screening, converter control interaction, and protection implications. RMS simulations are required for credible disturbances when the terminal SCR is moderate or high. EMT simulation is required when the export-side grid is weak, when grid-forming control is proposed, or when DC-fault recovery and fast converter control are central to the claim.

Frequency-Security Model

Let f_0 be the nominal frequency, H_{sys} the equivalent inertia constant on system baseS_{base}, and ΔP^{cont} the contingency power imbalance. Define the equivalent frequency-response mass as

$$M = \frac{2H_{\text{sys}}S_{\text{base}}}{f_0} \quad [\text{MW s/Hz}]. \tag{23}$$

A reduced frequency-response model is

$$M\frac{df(t)}{dt} = P^{\text{pri}}(t) + P^{\text{HVDC,FFR}}(t) + P^{\text{BESS,FFR}}(t) - \Delta P^{\text{cont}} - D_f(f(t) - f_0), \tag{24}$$

For reproducible nadir calculations, the numerical study must specify the load-damping coefficient, primary-response gain, response deadband (if any), activation delay, ramp rate, BESS/HVDC response capacity, saturation limits, and numerical integration step. If these parameters are not disclosed, the nadir values should be read as illustrative screening values rather than validated dynamic-simulation outputs.

where D_f is the load-damping coefficient in MW/Hz, $P^{\text{pri}}(t)$ is the primary frequency response, and $P^{\text{HVDC,FFR}}(t)$ and $P^{\text{BESS,FFR}}(t)$ are fast frequency-response injections from the HVDC controller and BESS, respectively.

At the instant after the disturbance, before the fast response and primary response act, the initial RoCoF is

$$\mathrm{RoCoF}_0 = -\frac{\Delta P^{\mathrm{cont}}}{M} = -\frac{f_0 \Delta P^{\mathrm{cont}}}{2H_{\mathrm{sys}} S_{\mathrm{base}}}. \tag{25}$$

The security constraints are

$$|\mathrm{RoCoF}_0| \le \mathrm{RoCoF}^{\max}, \tag{26}$$

$$\min_{0 \le t \le T^{\mathrm{sim}}} f(t) \ge f^{\min}, \tag{27}$$

$$R_{t\omega}^{\mathrm{pri}} + R_{t\omega}^{\mathrm{HVDC}} + R_{t\omega}^{\mathrm{BESS}} \ge \Delta P_{t\omega}^{\mathrm{cont}}. \tag{28}$$

A generic ramp-limited fast-response model can be represented as

$$P^{j,FFR}(t) = \begin{cases} 0, & t < T_j^{\mathrm{delay}}, \\ \min\left\{R_j,\ \rho_j\left(t - T_j^{\mathrm{delay}}\right)\right\}, & t \ge T_j^{\mathrm{delay}}, \end{cases} \qquad j \in \{\mathrm{HVDC}, \mathrm{BESS}\}, \tag{29}$$

where R_j, ρ_j, and T_j^{delay} are the response capacity, ramp rate, and activation delay of resource j.

For the stylised ELMED case, the reported base-case RoCoF follows directly from this model. With $f_0 = 50$ Hz, $\Delta P^{\mathrm{cont}} = 600$ MW, $H_{\mathrm{sys}} = 4.0$ s, and $S_{\mathrm{base}} = 10{,}000$ MVA,

$$|\mathrm{RoCoF}_0| = \frac{50 \times 600}{2 \times 4.0 \times 10{,}000} = 0.375 \text{ Hz/s}. \tag{30}$$

For the low-inertia case $H_{\mathrm{sys}} = 2.5$ s,

$$|\mathrm{RoCoF}_0| = \frac{50 \times 600}{2 \times 2.5 \times 10{,}000} = 0.600 \text{ Hz/s}. \tag{31}$$

These values are screening RoCoF values for the stylised case. They are useful for ranking candidate designs, but they do not replace RMS simulation of governor, BESS, HVDC control, and load-damping dynamics.

Voltage and Weak-Grid Screening

Converter terminals are screened using voltage limits, converter P-Q capability, and short-circuit ratio:

$$\mathrm{SCR}_k = \frac{SCC_k}{P_k^{\mathrm{conv}}}, \tag{32}$$

where SCC_k is the short-circuit capacity at terminal k, and P_k^{conv} is the converter active-power rating. When the converter's reactive-power capability is material, an effective short-circuit ratio may also be used:

$$E\mathrm{SCR}_k = \frac{SCC_k - Q_k^{\mathrm{comp}}}{P_k^{\mathrm{conv}}}. \tag{33}$$

TABLE III. Short-circuit-ratio screening for VSC-HVDC terminals

SCR range	Grid-strength interpretation	Required action
SCR >= 3	Strong grid	RMS dynamic study is normally adequate for screening.

2 <= SCR < 3	Moderate grid	Control sensitivity, N-1, and voltage-stability studies are required.
SCR < 2	Weak grid	An EMT study is required; consider grid-forming control, synchronous condensers, or additional AC reinforcement.

VSC-HVDC can support voltage, but the converter MVA rating, current saturation, outer-loop voltage control, PLL dynamics, and local AC grid strength limit this support. Therefore, converter support is treated as a constrained control resource rather than an unlimited stabilising device.

SCR and ESCR are early-stage indicators only. Converter-dominated stability also depends on the grid impedance angle, PLL bandwidth, current-saturation logic, outer-loop voltage control, grid-forming or grid-following mode, nearby converter interactions, protection settings, and harmonic performance. Designs near the weak-grid boundary, therefore, require EMT-level verification and not merely steady-state voltage or SCR reporting.

MARKET-COUPLING AND INVESTMENT-RECOVERY MODEL

An Africa-Europe HVDC link is both a physical asset and a market interface. The formulation below is a market-value indicator, not a complete European-African market-clearing engine. It separates energy arbitrage, loss-adjusted congestion rent, carbon value, reserve exchange, emergency support headroom, adequacy support, and long-term offtake arrangements. A full market study would require explicit bidding zones, capacity allocation rules, reserve product definitions, balancing market interfaces, carbon accounting, and contractual allocation of congestion rent.

$$\max W_{t\omega} = \sum_{d\in\mathcal{D}} U_d\left(P_{dt\omega}\right) - \sum_{g\in\mathcal{G}} C_g\left(P_{gt\omega}\right) - C^{\text{loss}} \sum_{k\in\mathcal{K}} P^{\text{loss}}_{kt\omega}. \tag{34}$$

The HVDC transfer constraint is

$$0 \le P^{\text{send}}_{kt\omega} \le \overline{P}^{\text{HVDC}}_{k} x_k. \tag{35}$$

Loss-adjusted congestion rent is computed as

$$CR_{kt\omega} = \lambda_{E,t\omega} P^{\text{rec}}_{kt\omega} - \lambda_{A,t\omega} P^{\text{send}}_{kt\omega}, \tag{36}$$

where $\lambda_{E,t\omega}$ and $\lambda_{A,t\omega}$ are the marginal prices in the European import zone and African export zone, respectively. If losses are neglected, this expression reduces to the common approximation

$$CR_{kt\omega} \approx \left(\lambda_{E,t\omega} - \lambda_{A,t\omega}\right) P^{\text{HVDC}}_{kt\omega}. \tag{37}$$

Expected annual congestion rent is

$$\mathbb{E}[CR_k] = \sum_{\omega\in\Omega} \pi_\omega \sum_{t\in\mathcal{T}} \Delta t \, CR_{kt\omega}. \tag{38}$$

The annual net benefit is

$$NB = \mathbb{E}[CR] + V^{\text{carbon}} + V^{\text{curtail}} + V^{\text{reserve}} + V^{\text{adequacy}} - C^{\text{ann.inv}} - C^{\text{O\&M}}, \tag{39}$$

and the benefit-cost ratio is

$$BCR = \frac{\mathbb{E}[CR]+V^{\text{carbon}}+V^{\text{curtail}}+V^{\text{reserve}}+V^{\text{adequacy}}}{C^{\text{ann.inv}}+C^{O\&M}}. \quad (40)$$

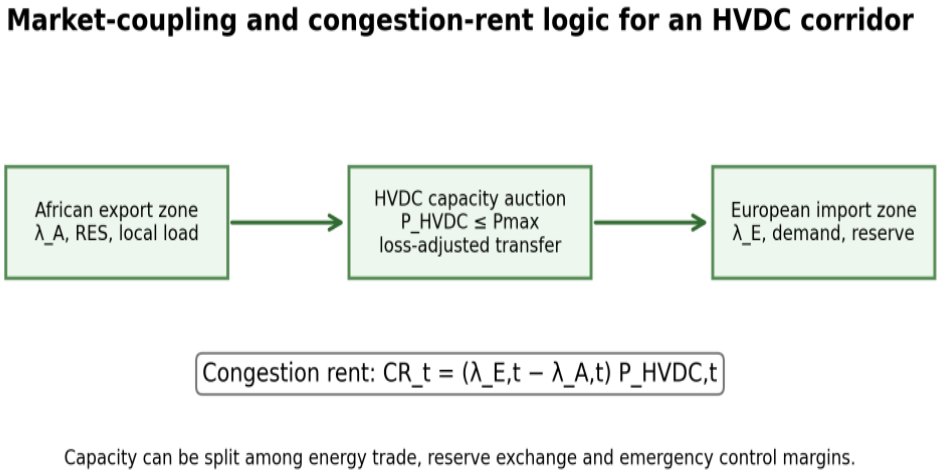


Fig. 5. *Market-coupling and congestion-rent logic for an Africa-Europe HVDC corridor.*

STYLISED ELMED-TYPE NUMERICAL CASE STUDY

A stylised ELMED-type Tunisia-Italy VSC-HVDC corridor is used to demonstrate the planning, security, and market indicators. The case is a screening benchmark, not an official project simulation. Its purpose is to show how the framework processes corridor capacity, storage-supported firming, HVDC losses, converter loading, RoCoF, frequency nadir, voltage security, and market sensitivity. The numerical values in Tables VI-IX are therefore interpreted as illustrative screening outputs, not as a fully reproducible utility-grade stochastic optimisation result.

For a Transactions-level submission, this section should be accompanied by supplementary data that includes the complete bus, line, generator, converter, renewable, BESS, load, price, cable availability, and contingency datasets. It should also report scenario-generation and scenario-reduction procedures, solver name and version, optimality gap, hardware, computation time, hourly dispatch outputs, AC/DC power-flow validation, RMS dynamic simulations for credible disturbances, and EMT validation for weak-grid converter terminals or DC-fault recovery. These requirements are stated explicitly to prevent overclaiming from a stylised case.

Case Description and Assumptions

TABLE IV. Stylised ELMED-type case assumptions and reproducibility status

Item	Assumption used in the illustrative case
HVDC corridor	Tunisia-Italy ELMED-type bipole VSC-HVDC link.
Rated transfer capacity	600 MW.
Approximate length	220 km, mostly submarine cable.
Converter rating	700 MVA per terminal for P-Q headroom.
Nominal frequency	50 Hz.
Export-side system base	10,000 MVA.
Base equivalent inertia	4.0 s; low-inertia sensitivity at 2.5 s.
Loss model	Approximately 3.7% total link losses in the base case, inferred from reported export and loss values; sensitivity should be stated explicitly in a reproducible implementation.
Renewable hub	1.2 GW solar plus 0.6 GW wind synthetic hourly profile.

Storage cases	0 MWh, 500 MWh, and 1000 MWh BESS cases.
Market-price spread	Base mean spread of 42 EUR/MWh, varied in sensitivity analysis.
Reproducibility status	Stylised screening dataset; final submission should provide complete network, scenario, solver, dispatch, AC/DC power-flow, RMS, and EMT validation files as supplementary material.

Synthetic Benchmark Dataset

To avoid ambiguity, the numerical case is supported by the synthetic benchmark dataset in Table V. The dataset is created solely for planning-level screening and to ensure reproducibility of the illustrative calculations. It is not an official ELMED project dataset, not confidential utility data, and not evidence of completed RMS or EMT validation. Verified utility data should therefore replace all network, scenario, cost, and dynamic quantities before an IEEE Transactions-level claim is made.

TABLE V. Synthetic benchmark dataset

Dataset block	Synthetic screening values	Purpose and replacement requirement
System base and zones	Base power: 10,000 MVA; nominal frequency: 50 Hz; export zone: North-Africa renewable hub; import zone: Italy/Europe market node; study horizon: representative 24 h, annualised for energy and rent indicators.	Defines a compact benchmark for screening. Replace with full multi-bus African and European network equivalents for a final submission.
Synthetic AC buses	A1: renewable hub, 220 kV; A2: export-side collector/PoC, 220 kV; A3: domestic-load bus, 220 kV; E1: European converter terminal, 400 kV; E2: import market/load bus, 400 kV.	Provides a minimal topology for AC/DC screening. Replace with complete bus names, voltage bases, shunts, transformer data, and regional equivalents.
Synthetic AC branches	A1-A2: 90 km, R = 0.018 p.u., X = 0.145 p.u., limit = 900 MW; A2-A3: 70 km, R = 0.015 p.u., X = 0.120 p.u., limit = 700 MW; E1-E2: 55 km, R = 0.010 p.u., X = 0.090 p.u., limit = 1200 MW.	Allows reproducible screening of export-side and import-side AC constraints. Replace with verified line/cable/transformer impedances and thermal ratings.
Synthetic generation and demand	Dispatchable export-side unit at A3: Pmin = 100 MW, Pmax = 850 MW, cost = 55 EUR/MWh, inertia H = 4.0 s, droop = 5%; domestic demand: 700-1100 MW over the representative day; import-zone demand proxy: 2000-3200 MW.	Represents adequacy protection and price-zone demand in reduced form. Replace with chronological data on demand, generator cost, ramp, reserve, and inertia.
Renewable hub	Solar PV at A1: 1200 MW installed; wind at A1: 600 MW installed; representative capacity-factor envelope: solar 0-0.92, wind 0.18-0.58, with curtailment allowed at a penalty of 5 EUR/MWh.	Supports renewable-export and curtailment indicators. Replace with measured or public renewable time series and documented scenario-generation methods.
VSC-HVDC corridor	Bipole VSC-HVDC between A2 and E1; transfer rating: 600 MW in base cases and 1000 MW in reinforcement sensitivity; converter rating: 700 MVA per terminal; base total link loss: 3.7%; converter P-Q operation constrained by apparent-power and current limits.	Supplies a transparent converter/cable screening model. Replace with detailed converter controls, loss curves, DC voltage/current limits, and protection assumptions.
BESS cases	B0: 0 MW/0 MWh; B1: 250 MW/500 MWh, round-trip efficiency 88%; B2: 500 MW/1000 MWh, round-trip efficiency 88%; SOC range: 10-	Enables comparison of no-storage, medium-storage, and reinforced-storage export firming.

	90%; initial and terminal SOC: 50%.	Replace with vendor- or project-specific BESS ratings and degradation assumptions.
Scenario set	S1 high RES/low demand/high spread, probability 0.25; S2 base RES/base demand/base spread, probability 0.40; S3 low RES/high demand/high local adequacy stress, probability 0.25; S4 cable derating/low availability, probability 0.10.	Provides an auditable stochastic screening set. Replace with statistically justified scenario generation and scenario reduction.
Market and adequacy parameters	Base price spread: 42 EUR/MWh; low-spread sensitivity: 25 EUR/MWh; carbon value sensitivity: +30 EUR/MWh; domestic adequacy floor: domestic demand plus 15% upward reserve margin before export.	Allows the market-value and adequacy-protection logic to be reproduced. Replace with market-clearing data, reserve products, carbon accounting rules, and offtake assumptions.
Security-screening parameters	HVDC pole-outage contingency: 600 MW; base inertia: 4.0 s; low-inertia sensitivity: 2.5 s; minimum nadir criterion: 49.5 Hz; maximum RoCoF screening threshold: 0.5 Hz/s; fast response cases: 200 MW and 300 MW.	Supports planning-level frequency screening only. Replace with RMS and EMT models before claiming dynamic validation.

This synthetic dataset deliberately exposes the assumptions behind the illustrative ELMED-type case. It is sufficient for screening the planning logic, adequacy constraint, BESS-firming effect, cable-loss treatment, RoCoF calculation, and price-spread sensitivity. It is not sufficient for the final project design because it lacks detailed converter control parameters, protection settings, measured renewable traces, validated AC grid equivalents, or time-domain dynamic models.

Planning and Market Results

TABLE VI. Screening planning and market outcomes for the stylised ELMED-type case

Case	HVDC capacity	BESS energy	Annual export	Renewable curtailment	HVDC losses	Annual congestion rent	Planning interpretation
C0: no export link	0 MW	0 MWh	0.00 TWh	18.00%	0.00 TWh	0 MEUR	Baseline with high curtailment and no cross-border value.
C1: ELMED link only	600 MW	0 MWh	3.75 TWh	9.80%	0.139 TWh	158 MEUR	Economically useful, but export is less firm.
C2: ELMED + firming	600 MW	500 MWh	4.51 TWh	4.30%	0.167 TWh	189 MEUR	Preferred medium-scale option; curtailment and ramping improve.
C3: reinforced export	1000 MW	1000 MWh	6.16 TWh	2.10%	0.246 TWh	246 MEUR	Higher value but requires AC reinforcement and a stronger converter terminal.

The screening numerical results indicate that storage-supported firming increases export utilisation and reduces renewable curtailment. For the 600 MW corridor, the theoretical maximum annual transfer is

$$E_{\max} = 600 \times 8760 = 5.256 \text{ TWh/year.} \quad (41)$$

Thus, the original 600 MW results correspond to utilisation levels of approximately

$$\frac{3.75}{5.256} = 71.3\%, \qquad \frac{4.51}{5.256} = 85.8\%. \tag{42}$$

The movement from C1 to C2 demonstrates the operational value of storage-supported export firming. The movement from C2 to C3 increases exports and further reduces curtailment, but it also requires a higher converter rating, stronger AC-grid support, and additional voltage-security verification. The renewable profiles, BESS dispatch schedules, export schedules, and curtailment calculations should be reported in an appendix or supplementary file before the case is presented as reproducible science. Maximum cable capacity is not automatically the optimal planning decision.

Power-Flow and Voltage-Security Indicators

TABLE VII. Screening AC/DC power-flow and voltage-security indicators

Operating condition	Export transfer	Converter P-Q loading	Export-side voltage	Import-side voltage	Security comment
Base export, high RES	580 MW	0.83 p.u. MVA	0.992 p.u.	1.004 p.u.	Secure.
Peak export, low local load	600 MW	0.88 p.u. MVA	0.985 p.u.	1.006 p.u.	Secure with voltage control.
N-1 AC corridor outage	540 MW derated	0.81 p.u. MVA	0.964 p.u.	1.002 p.u.	Secure only after transfer derating.
Weak-grid sensitivity	600 MW	0.91 p.u. MVA	0.947 p.u.	1.005 p.u.	Requires reinforcement or grid-forming control.

The voltage-security indicators show that the base- and peak-export cases remain within the assumed voltage range under converter-voltage control. The N-1 case is feasible only after transfer derating. The weak-grid sensitivity approaches the lower voltage-security boundary and therefore requires AC reinforcement, grid-forming control, or additional dynamic validation. A final submission must state the voltage limits, identify the export- and import-side buses, describe the converter control assumptions, and validate the operating points using AC/DC power-flow analysis.

Frequency Response

TABLE VIII. Illustrative frequency-security screening results for HVDC pole outage

Disturbance	Fast support	Initial RoCoF	Frequency nadir	Recovery by 25 s	Secure?
Loss of 600 MW HVDC pole	None	0.375 Hz/s	49.48 Hz	49.95 Hz	Marginal; violates 49.5 Hz criterion.
Loss of 600 MW HVDC pole	200 MW BESS/HVDC fast response	0.250 Hz/s	49.66 Hz	49.98 Hz	Secure.
Loss of 600 MW pole, low inertia (H = 2.5 s)	None	0.600 Hz/s	49.31 Hz	49.90 Hz	Not secure.
Low inertia with grid-forming/BESS response	300 MW fast response	0.300 Hz/s	49.61 Hz	49.97 Hz	Secure after control support.

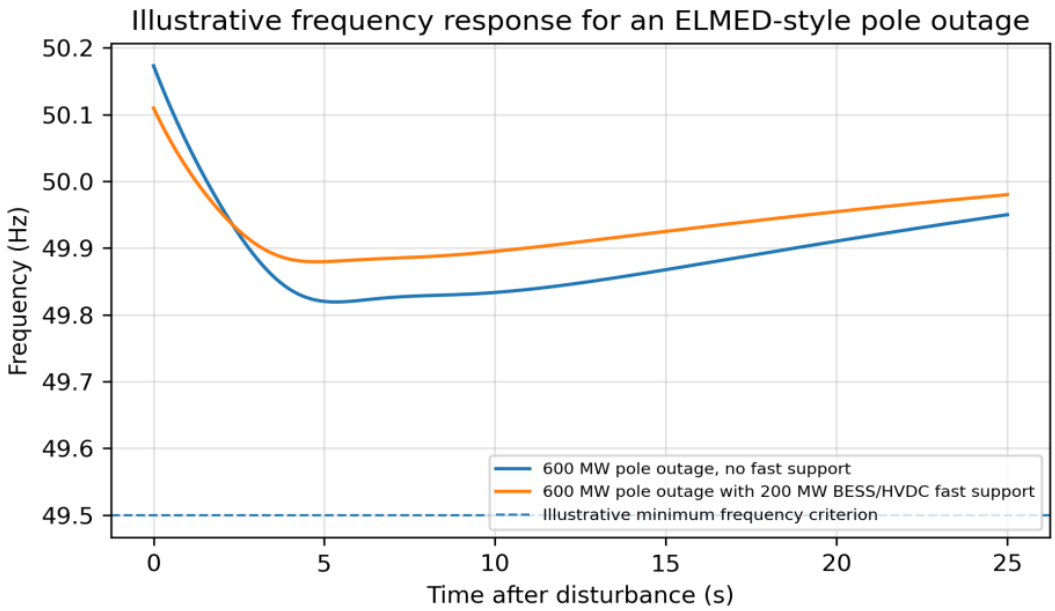


Fig. 6. *Illustrative frequency response after a 600 MW HVDC pole outage with and without fast support.*

The frequency screening results show that a 600 MW pole outage can become a binding frequency-security constraint. Without fast support, the base case reaches an illustrative nadir of 49.48 Hz, violating the 49.5 Hz criterion. With 200 MW of BESS/HVDC fast response, the nadir improves to 49.66 Hz. In the low-inertia case, the initial RoCoF rises to 0.600 Hz/s, and the nadir falls to 49.31 Hz, so additional grid-forming or BESS response is required. These nadir and recovery values should be supported by a fully specified reduced-order model or RMS simulation before being used as validated dynamic results.

Sensitivity Analysis

TABLE IX. Sensitivity results and engineering interpretation for the stylised case

Sensitivity case	Change applied	Effect on annual net benefit	Engineering implication
Cable cost increase	+30% annualised cable cost	Benefit-cost ratio falls from 1.34 to 1.08.	Project remains marginal; offtake contract becomes critical.
Lower cable availability	98% to 92% availability	Export energy falls by 0.27 TWh/year.	Repair logistics and redundancy affect bankability.
Higher carbon value	Carbon value +30 EUR/MWh	Annual value increases by about 92 MEUR.	Carbon accounting strongly affects market case.
Low market spread	Mean spread 42 to 25 EUR/MWh	Congestion rent falls by about 40%.	Market design cannot be ignored.
Weak-grid terminal	SCR falls below 2	Voltage margin becomes insufficient.	Requires EMT study, reinforcement, or grid-forming VSC.

The sensitivity results confirm that project feasibility cannot be inferred from transfer capacity alone. Availability, grid strength, carbon value, and price-spread persistence significantly influence technical and commercial value. The ranges used for cable cost, cable availability, carbon value, price spread, and SCR should be justified from project data, public statistics, peer-reviewed literature, or clearly labelled expert assumptions.

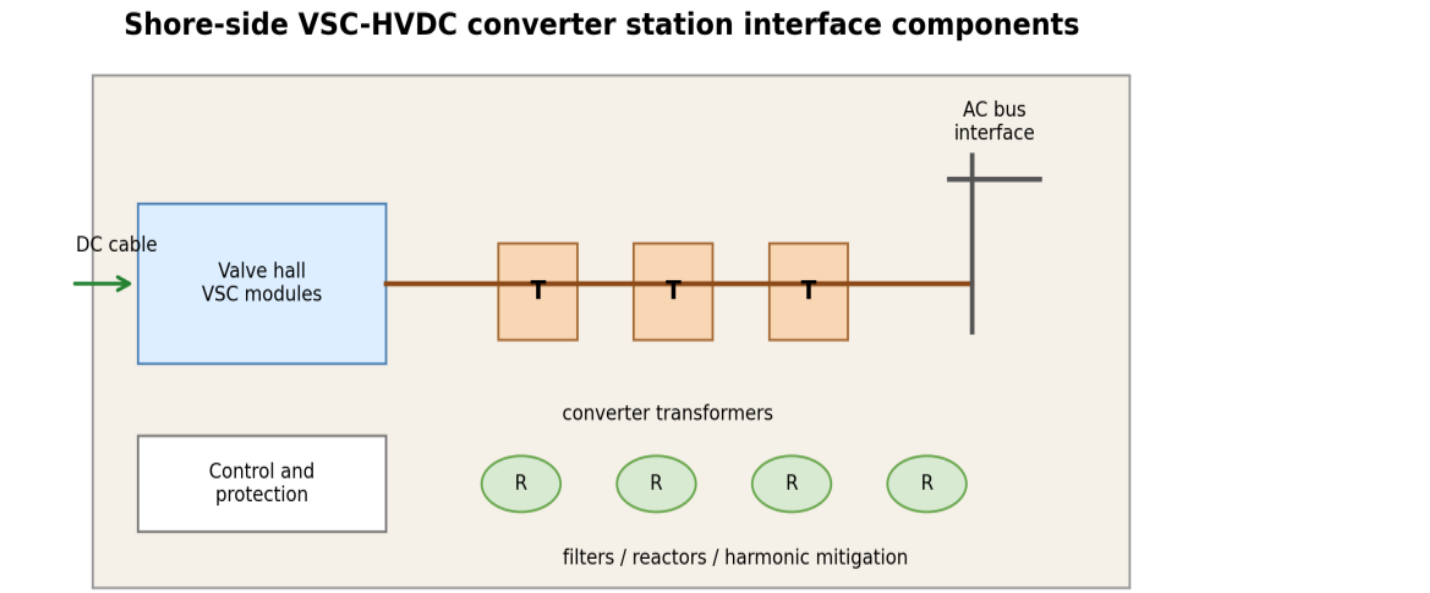


Fig. 7. *Shore-side VSC-HVDC converter-station interface components required for AC/DC integration studies.*

DISCUSSION

The proposed framework leads to five engineering observations.

First, domestic adequacy in the exporting African grid must be protected explicitly. The adequacy constraint prevents export schedules from consuming local reliability margin. This is not merely a political consideration; it is a power-system security constraint.

Second, VSC-HVDC can support voltage and frequency, but only within converter-current and control limits. Treating converter support as unlimited is a modelling error. The converter MVA rating, current limit, P-Q capability, PLL or grid-forming control design, and local short-circuit strength must all be represented.

Third, storage is not merely an optional commercial asset. In the stylised ELMED-type results, BESS-supported firming improves utilisation, reduces curtailment, and supplies fast frequency response. This makes storage a technical device for export firming, ramp limitation, and frequency security.

Fourth, market integration must be co-designed with operational security. Energy schedules, emergency margins, and reserve capacity compete for the same HVDC transfer capability. A corridor that maximises day-ahead energy arbitrage may not leave adequate headroom for emergency support.

Fifth, weak-grid operation requires more than SCR screening. SCR is useful for early-stage planning, but final claims about stability require RMS and, where necessary, EMT-level validation. This is especially important for African collector grids with low short-circuit strength, high converter penetration, and limited synchronous inertia.

CONCLUSION

This paper models the Africa-Europe VSC-HVDC renewable electricity trade as a coupled stochastic planning and screening challenge, addressing AC/DC operation, frequency and voltage security, and market evaluation. It separates non-anticipative first-stage investment choices from scenario-specific dispatch, explicitly incorporates AC/DC and converter constraints, safeguards domestic adequacy in Africa's export sector, and relates physical transfer to congestion rent and investment recovery metrics, adjusted for losses. The synthetic screening dataset clearly labels results, showing that a 600 MW VSC-HVDC corridor can cut renewable curtailment, boost annual exports, and generate congestion rent. Storage-backed firming enhances utilization from about 71.3% to 85.8% in the 600 MW case and improves frequency-response results after a 600 MW

pole outage. The findings also indicate that transfer capacity alone is insufficient as a planning metric. Converter P-Q limits, AC-grid strength, frequency-response resources, local adequacy safeguards, market-price spreads, carbon value, and cable availability are equally important design constraints. Future research should incorporate utility-grade network models, open scenario data, reproducible optimization code, RMS/EMT validation, and comprehensive market simulations.

REFERENCES

1. European Commission, "ELMED Electricity Interconnection in Tunisia," Global Gateway, accessed Jun. 27, 2026.
2. Terna, "ELMED: MASE authorises the Italy-Tunisia interconnection," Press Release, May 15, 2024.
3. European Commission, "GREGY - High Voltage Electrical Interconnection in the Eastern Mediterranean," Global Gateway, accessed Jun. 27, 2026.
4. GREGY Interconnector, "Electrical Interconnection Project," accessed Jun. 27, 2026.
5. Red Electrica de Espana, "Electricity link Spain-Morocco," Press Release, Sep. 4, 2020.
6. Redeia, "Spain and Morocco agree on the development of a third interconnection between both countries," Press Release, Feb. 14, 2019.
7. O. Apata, A. V. Adebayo and P. K. Ainah, "Renewable Energy Systems and The Fourth Industrial Revolution," 2021 IEEE PES/IAS PowerAfrica, Nairobi, Kenya, pp. 1–5, Aug 2021.
8. Reuters, "Britain shuns $34 billion Morocco-UK subsea power project," Jun. 26, 2025.
9. P. Kundur et al., "Definition and classification of power system stability, IEEE/CIGRE joint task force on stability terms and definitions," IEEE Trans. Power Syst., vol. 19, no. 3, pp. 1387-1401, Aug. 2004.
10. N. Flourentzou, V. G. Agelidis, and G. D. Demetriades, "VSC-based HVDC power transmission systems: An overview," IEEE Trans. Power Electron., vol. 24, no. 3, pp. 592-602, Mar. 2009.
11. M. P. Bahrman and B. K. Johnson, "The ABCs of HVDC transmission technologies," IEEE Power Energy Mag., vol. 5, no. 2, pp. 32-44, Mar.-Apr. 2007.
12. A. J. Conejo, L. Baringo, S. J. Kazempour, and A. S. Siddiqui, Investment in Electricity Generation and Transmission: Decision Making under Uncertainty. Cham, Switzerland: Springer, 2016.
13. A. J. Conejo, M. Carrion, and J. M. Morales, Decision Making Under Uncertainty in Electricity Markets. New York, NY, USA: Springer, 2010.
14. ENTSO-E, "High Voltage Direct Current links in system operations," System Operations Report, 2019.
15. D. Van Hertem and M. Ghandhari, "Multi-terminal VSC HVDC for the European supergrid: Obstacles," Renew. Sustain—Energy Rev., vol. 14, no. 9, pp. 3156-3163, 2010.
16. D. Jovcic and K. Ahmed, High Voltage Direct Current Transmission: Converters, Systems and DC Grids. Hoboken, NJ, USA: Wiley, 2015.
17. J. Beerten, S. Cole, and R. Belmans, "A sequential AC/DC power flow algorithm for networks containing multi-terminal VSC HVDC systems," IEEE Trans. Power Syst., vol. 27, no. 2, pp. 821-829, May 2012.
18. M. K. Bucher and C. M. Franck, "Fault current interruption in multiterminal HVDC networks," IEEE Trans. Power Del., vol. 31, no. 1, pp. 87-95, Feb. 2016.
19. J. Renedo, A. Garcia-Cerrada, and L. Rouco, "Active power control strategies for transient stability enhancement of AC/DC grids with VSC-HVDC multi-terminal systems," IEEE Trans. Power Syst., vol. 31, no. 6, pp. 4595-4604, Nov. 2016.
20. R. Eriksson, N. Modig, and K. Elkington, "Synthetic inertia versus fast frequency response: A definition," IET Renew. Power Gener., vol. 12, no. 5, pp. 507-514, 2018.
21. R. Romero, A. Monticelli, A. Garcia, and S. Haffner, "Test systems and mathematical models for transmission network expansion planning," IEE Proc.-Gener. Transm. Distrib., vol. 149, no. 1, pp. 27-36, Jan. 2002.
22. J. Choi, T. D. Mount, R. J. Thomas, and R. Billinton, "Probabilistic reliability criterion for planning transmission system expansions," IEE Proc.-Gener. Transm. Distrib., vol. 153, no. 6, pp. 719-727, Nov. 2006.
23. L. Baringo and A. J. Conejo, "Transmission and wind power investment," IEEE Trans. Power Syst., vol. 27, no. 2, pp. 885-893, May 2012.
24. A. Moreira, A. Street, and J. M. Arroyo, "An adjustable robust optimisation approach for contingency-

constrained transmission expansion planning," IEEE Trans. Power Syst., vol. 30, no. 4, pp. 2013-2022, Jul. 2015.
25. J. Z. Zhou, H. Ding, S. Fan, Y. Zhang, and A. M. Gole, "Impact of short-circuit ratio and phase-locked-loop parameters on the small-signal behaviour of a VSC-HVDC converter," IEEE Trans—Power Del., vol. 29, no. 5, pp. 2287-2296, Oct. 2014.
26. H. Saad, S. Dennetiere, J. Mahseredjian, P. Delarue, X. Guillaud, J. Peralta, and S. Nguefeu, "Modular multilevel converter models for electromagnetic transients," IEEE Trans. Power Del., vol. 29, no. 3, pp. 1481-1489, Jun. 2014.
27. D. Van Hertem, O. Gomis-Bellmunt, and J. Liang, HVDC Grids: For Offshore and Supergrid of the Future. Hoboken, NJ, USA: Wiley, 2016.
28. Adeyinka Victor Adebayo, Hussein Kehinde Adebayo, Samuel Oladeji, "Implementing Electrical Energy Storage for Improved Voltage Stability in Power Systems with Substantial Wind Generation., vol. 14, pp. 57-66, Mar. 2024.
29. H. Bevrani, Robust Power System Frequency Control. New York, NY, USA: Springer, 2009.
30. N. Hatziargyriou et al., "Definition and classification of power system stability - revisited and extended," IEEE Trans. Power Syst., vol. 36, no. 4, pp. 3271-3281, Jul. 2021.